

Evolution of the Arctic stratospheric aerosol mixing ratio measured with balloon-borne aerosol backscatter sondes for years 1988 - 2000

T. Suortti,¹ J. Karhu,¹ R. Kivi,¹ E. Kyrö,¹ J. Rosen,² N. Kjome,² N. Larsen,³ R. Neuber,⁴ V. Khattatov,⁵ V. Rudakov,⁵ V. Yushkov,⁵ and H. Nakane⁶

Abstract. Balloon-borne aerosol backscatter measurements were made at 12 Arctic stations as part of a polar stratospheric cloud study. The record starts in 1988, which is well before the eruption of Mount Pinatubo in the beginning of June 1991, and continues to 2000. These measurements provide absolutely calibrated in situ detection of atmospheric aerosols with simultaneous measurements of pressure, temperature, relative humidity, and O₃ partial pressure. The instrument is also capable of operating during cloudy conditions, which may be considered as an advantage compared with lidar measurements. Even though backscatter soundings represent the state of the atmosphere at the sounding time and site, we demonstrate here that with a limited, homogeneous set of measurements it is possible to effectively study the time development of atmospheric aerosol loading. The initial aim of the study has been to define the general features of aerosol distribution in the Arctic winter troposphere and stratosphere and then to document the perturbation in the lower stratospheric aerosols caused by the eruption of Mount Pinatubo and, in addition, to infer the background state of lower stratospheric aerosol loading during the pre- and post-Pinatubo conditions. Our measurements suggest that the *e*-folding time for the decaying volcanic aerosol intrusion was ~0.7 year and the full recovery of the Arctic lower stratosphere from the Mount Pinatubo perturbation was roughly 5 years.

1. Introduction

Recent studies [WMO, 1999] have shown that concentration, size, and phase of the stratospheric aerosols, i.e., stratospheric sulfate aerosol (SSA) and polar stratospheric clouds (PSCs), have a crucial effect on the stratospheric ozone chemistry. SSA abundance is affected strongly by volcanic activity, and hence it is characterized by transient changes. The perturbation in SSA abundance induced by the eruption of Mount Pinatubo and also the pre- and post-Pinatubo periods are used here to investigate the natural changes and the recent state of the lower stratospheric aerosol loading.

Aerosols also affect the radiative balance of the Earth. Aerosol radiative forcing may be described as working in two ways, directly and indirectly. The direct aerosol effect is

associated with scattering and absorption of solar radiation, while the indirect effect is related to the influence of aerosols on nucleation and microphysical properties of clouds, which could modify cloud evolution and albedo. The most recent estimates [International Panel on Climate Change, 2001] on the present understanding of aerosol-induced radiative forcing suggest that the overall effect of direct forcing is about -0.2 W/m^2 with large error margins. The indirect effect of tropospheric aerosols is estimated to be in the range of 0 to -2 W/m^2 . The large uncertainties are related to the lack of basic information needed for making the required calculations or estimates. The measurements reported here were conducted with the expectation of advancing the understanding of Arctic region aerosols and associated climate forcing issues in both the troposphere and stratosphere.

2. Methods

Our measurements provide aerosol backscatter profiles from ground level to ~27 km or 15 hPa. In the backscatter sonde, two photometers operating at 940 nm and 490 nm are used to detect locally backscattered light from a collimated xenon flash lamp beam. The flash is triggered at ~7-s intervals. The light intensity measured with the photometers is normalized by the pure molecular scattering signal (Rayleigh scattering), which is determined by calibration against a standard instrument similar to the backscatter sonde but which is different in that it can be calibrated in

¹Finnish Meteorological Institute, Arctic Research Centre, Sodankylä, Finland.

²Department of Physics and Astronomy, University of Wyoming, Laramie, Wyoming, USA.

³Division of Middle Atmosphere Research, Danish Meteorological Institute, Copenhagen, Denmark.

⁴Alfred Wegner Institute, Potsdam, Germany.

⁵Central Aerological Observatory, Moscow, Russia.

⁶National Institute of Environmental Studies, Tsukuba, Japan.

Copyright 2001 by the American Geophysical Union.

Paper number 2000JD000180.
0148-0227/01/2000JD000180\$09.00

a chamber flushed with aerosol-free air. The data product achieved in this way is the backscatter ratio (BSR). The BSR is close to unity in clean atmospheric conditions and may be more than 2 magnitudes greater in strong PSCs. The intensity of backscattered light from atmospheric aerosols alone is derived from BSR by subtracting 1 from it and is denoted here as the aerosol backscatter ratio (ABSR). For typically reported atmospheric aerosol size distributions the ABSR is roughly a linear function of the aerosol mass loading [Rosen and Kjome, 1991] and has the properties of a mixing ratio parameter. The final data product has a vertical resolution of ~ 30 m and a 1% random noise component in the troposphere, which increases gradually to $\sim 5\%$ at the top of the sounding.

By using the measured ABSR, it is possible to estimate the stratospheric aerosol mass and aerosol surface area. For inferring the aerosol mass, a robust conversion method was described by Rosen *et al.* [1994], which is based on ensembles of published size distributions measured under diverse stratospheric conditions. Scatterplots relating the aerosol mass and backscatter for the red channel have been illustrated [Rosen and Kjome, 1991; Rosen *et al.*, 1992, 1993]. Stevermer *et al.* [2000] have conveniently documented these ensemble size distributions and illustrated their usefulness for other calculations. The interested reader can find them at the National Oceanic and Atmospheric Association Surface Radiation Research Branch web site (<http://www.srrb.noaa.gov/research/aerosol.html>). The scatterplots themselves suggest an overall conversion uncertainty of about $\pm 15\%$. Additional uncertainties may arise from variable particle composition, but this is thought to be of a fairly minimum consequence for our application. The conversion from ABSR at 940 nm to aerosol mass is given by

$$\text{MMR}(\text{ppbm}) = 4.14(\text{ABSR}_{940})^{0.8823}, \quad (1)$$

where MMR (ppbm) is the aerosol mass mixing ratio in parts per billion by mass and ABSR_{940} is the aerosol backscattering ratio at 940 nm. In addition to the conversion for the mass mixing ratio, a conversion for aerosol surface area was also developed by Rosen *et al.* [1994]. The conversion from ABSR to aerosol surface area is given by

$$A = 30.8(\text{ABSR}_{940})^{0.6165}, \quad (2)$$

where A is the aerosol surface area in $\mu\text{m}^2/\text{mg}$ of air and ABSR_{940} is as previously defined. It should be noted that these conversions from ABSR_{940} to MMR and A introduced above reflect the aerosol mass (or area) variations insofar as the measured size distributions reflect the true size distributions and associated variations. These conversions are developed for the midlatitude stratospheric conditions, and applying them in the case of Arctic soundings may introduce some error to the calculated aerosol loading properties, but, as mentioned above, this has a fairly insignificant effect.

The application of two widely different wavelengths provides an approximate but often useful tool for size estimation of the scattering aerosols. The size information can be in-

ferred from a color index (CI), which is calculated from the ABSR by dividing the aerosol signal in the 940-nm channel by the aerosol signal in the 490-nm channel. There have been several studies illustrating the CI response to various aerosol size distributions [Rosen and Kjome, 1991; Rosen *et al.*, 1994, 1997a, b; Larsen *et al.*, 1997]. For extreme values the CI is 1.00 in the small-particle limit and is ~ 15 in the large-particle limit. For free tropospheric aerosols a range in CI from 7 to 12 corresponds to spherical particle radii ranging from ~ 250 to 2000 nm, respectively. For near-background stratospheric aerosols the CI values are typically in the range of 4-6. It should be noted that CI is a rather rough measure for estimating the size of the scattering particles. The error in CI increases especially at high altitudes and with small, near-background, ABSR values.

3. Measurements

In this study we have made use of an extensive Arctic backscatter sonde database. The data set consists of soundings made at 12 different Arctic locations, which are shown in the map in Figure 1. All of the soundings have been conducted during the winter months and after sunset. Most of them were made inside of the winter polar vortex. In this study both ascending and descending data were available. However, since the ascent and descent profiles are almost identical (except for cloud structure), only the ascent profiles are shown here.

All of the data were passed through a final analysis at the University of Wyoming, where outliers and noise spikes not confirmed by descent data were removed. In addition, a small calibration adjustment for the 490-nm channel was made in order to gain consistent and slowly changing strato-

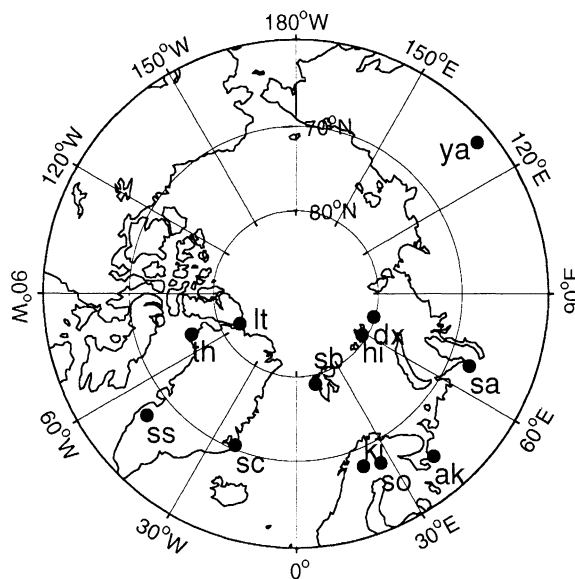


Figure 1. Map of the Arctic sounding sites. Abbreviations for station names are as follows: so, Sodankylä; ki, Kiruna; th, Thule; ya, Yakutsk; sb, Ny Ålesund; sc, Scoresby Sund; ss, Søndre Strømfjord; ak, Arkangel'sk; It, Alert; dx, Dixon Island; hi, Heiss Island; and sa, Salekhard.

spheric CI values. It is characteristic for the 490-nm channel to have a very low backscatter ratio when low aerosol concentrations are encountered, and in such a case it may even drop under unity. This may happen because of a natural uncertainty in the measurement, or it can be caused by a small calibration change in the instrument. The adjustments, which have been made for the 490-nm channel to eliminate nonphysical backscatter ratios, have been in the range of 0-4%. This effect has been documented in more detail by *Rosen et al.* [1997a]. Saturated signal values caused by clouds have been removed in the most obscuring cases, but some can still be identified visually in the plots as blue tracks in the tropospheric part of the soundings. A total of 151 profiles was used in this study.

4. Results and Discussion

Vertical ABSR profiles derived from backscatter sondes have been described earlier by *Rosen et al.* [1997a] for midlatitude measurements at Lauder, New Zealand, and Laramie, Wyoming. We present in Plates 1 and 2 the vertical ABSR₉₄₀ and CI profiles of 12 successive Arctic winters. It may be noted that because the soundings were always made in relatively calm conditions during the wintertime (November to March) and after sunset, the profiles may be biased to such conditions.

The most pronounced features in the profiles are clouds. Both tropospheric and stratospheric clouds are clearly distinguishable by the sudden rise in backscatter values. The ABSR₉₄₀ is roughly 1-2 magnitudes higher inside clouds compared with the background value. Also, higher CI values are observed inside clouds (if the signal is not saturated), which give a clear indication of increased particle size. CI is observed to approach 15 in clouds, which can be interpreted as a presence of large particles, i.e., cloud particles, with diameters of several microns or larger. In the cases of low- and middle-level clouds the backscatter signal is often too strong, and the measurement becomes saturated. This is observed in Plates 1 and 2 as uniformly rising traces with a high ABSR₉₄₀ and low CI values (see the lower right quadrant of the 1991-1992 winter frame in Plate 1). In the process of making ABSR₉₄₀ profiles more informative, the most obscuring saturation cases have been removed from the plots.

By visually ignoring cloud anomalies, the general structure of the Arctic atmosphere can be identified in the vertical ABSR₉₄₀ profiles. There are some general features in ABSR₉₄₀ profiles that are characteristic for certain parts of the atmosphere. These features are briefly described as follows: The lowest part of the ABSR profile is characterized by a footlike structure, which represents the planetary boundary layer (PBL). In the PBL the ABSR is observed to decrease with height concurrent with a reduction in particle size as implied by the CI. In the PBL both the ABSR and CI variations are observed to be larger than in the free troposphere. An ABSR minimum is observed directly above the PBL, which also correlates with small CI values. Even though this feature tends to be obscured by the clouds in

most of the plots in Plates 1 and 2, the minimum is evident in single soundings with minimal or no clouds. The exact height of the tropopause is not obvious from these ABSR₉₄₀ plots, and for the sake of clarity it should be mentioned that in the majority of soundings the temperature tropopause is located between 200 and 350 hPa.

In general, the stratospheric portion of the profiles is often characterized by conditions of significant PSC activity. Under conditions of high PSC activity the stratospheric ABSR is characterized by strong positive anomalies. Under conditions of no PSC activity the ABSR probably indicates background values characteristic of the isolated vortex. Soundings made outside of the polar vortex differ from the latter ones by displaying somewhat higher background levels for the stratospheric ABSR.

If PSCs are ignored, the stratospheric aerosol mixing ratio is observed to have a maximum at an ~50- to 200-hPa height interval, and above this level the aerosol mixing ratio will start to diminish with altitude. The average particle size, according to CI calculations, is observed to have a similar behavior with altitude as the aerosol mixing ratio.

In the lower stratosphere, between ~100 and 200 hPa, which corresponds to ~12-16 km, it is possible to distinguish a relatively consistent and uniform ABSR profile with minimal disturbance from PSCs or cirrus clouds. This range, at least the upper end of it, is always near the stratospheric aerosol maximum. It may be suggested that this region represents the typical or characteristic undisturbed aerosol loading for the associated year, and therefore it is a good region for deducing the time development of lower stratospheric aerosol mass loading and identifying the volcanic aerosol perturbation caused by the Mount Pinatubo eruption.

By examining the change of altitude of the aerosol maximum with time, it is possible to see the diabatic descent of air mass during the winter. The soundings made in late winter and inside the vortex represent cases where the maximum has shifted somewhat downward compared with the early winter soundings. This feature is seen better when examining single soundings (not shown here). It is also observed that the height of the maximum in the measured aerosol loading during the Pinatubo perturbation is decreasing with time when comparing successive winters, which is most likely due to the subsidence of volcanic aerosol. Inferring the characteristic subsidence rates for the volcanic aerosol intrusion was not within the scope of this paper.

If these 12 successive winters are compared (see Plates 1 and 2), the following characteristics are readily apparent: First of all, there is an indication of elevated ABSR background levels in the lower stratosphere during the winters 1991-1992 to 1995-1996. It would also seem that during those winters, somewhat higher CI values are recorded in the same region. In this region, CI is expected to vary between 4 and 6, but during the Pinatubo perturbation, CI seems to vary more likely between 6 and 8. This may be interpreted as an increased size of the scattering aerosols.

To test the former propositions, we calculated annual averages of the ABSR and CI data at given altitudes in order

to reduce the fine structure and statistical noise so that a true variation in the background would become more apparent. As mentioned earlier, the range of 100-200 hPa is well suited for this kind of examination. The averaging was done by taking 10-hPa boxes along the profile. The result of ABR averaging is shown in Plate 3, where the seasonal averages of 940-nm ABR profiles are plotted within the 100- to 200-hPa levels. Plate 3 demonstrates the evolution of aerosol loading in the study region and suggests that the evolution of the aerosol loading in this region follows the expected course set by the Pinatubo event. All winters from 1988-1989 to 1999-2000 are included. The 1988-1989 to 1990-1991 winters represent, obviously, the background state before the Pinatubo perturbation. An increased amount of volcanic aerosol is observed for the first time during the 1991-1992 winter (red line). The graph suggests how the layer of volcanic aerosol descends or evolves in the lower stratosphere. As can be noted, the maximum concentration of Pinatubo aerosols is still above the study region during the 1991-1992 winter. The former conclusion can be drawn when viewing the complete profiles (Plates 1 and 2) and the gradients of averaged $ABSR_{940}$ profiles in Plate 3. The Pinatubo perturbation is observable until the 1995-1996 winter, after which the lower stratospheric aerosol loading seems to settle back to the unperturbed background state.

Figure 2a shows the averages of the $ABSR_{940}$ profiles in Plate 3 as a function of time. For viewing convenience the points have been connected by a solid line, which should not be interpreted as necessarily representing the actual conditions between measurements. It may be noted that the average values of the profiles are a measure of the net aerosol loading in the chosen altitude range. Thus Figure 2a more quantitatively illustrates the time evolution of lower stratospheric aerosol loading in the lower stratosphere. The aerosol mass mixing ratio and surface area, resulting from equations (1) and (2), are presented in Figures 2b and 2c, respectively. Although the eruption of Mount Pinatubo took place in June 1991, the peak in the aerosol backscatter was not observed until the 1992-1993 winter (soundings were made only during the winter), when the maximum value for the seasonally averaged $ABSR_{940}$ was 6.70, which corresponds to the peak aerosol mass of 99 ppb and aerosol surface area of $22 \mu\text{m}^2/\text{mg}$. Apparent background levels before and after the Pinatubo event seem to match quite well within the range of natural variation. As can be noted in the Figure 2a, the apparent background value for $ABSR_{940}$ is ~ 0.30 . Background values for aerosol mass and surface area are ~ 1 ppb and $15 \mu\text{m}^2/\text{mg}$, respectively, which are plotted in the Figures 2b and 2c with dashed lines as a marker for the background level during the Pinatubo event. However, there is a possibility that the long-term background value could be somewhat lower than during the very last years before the eruption of Mount Pinatubo. This is suggested by the slightly decreasing trend in ABR after the Pinatubo event. Continuation of the time series and a better evaluation of near-background variations are needed to decisively settle this question.

The decay rate of the Pinatubo perturbation itself can be estimated by subtracting the background value (0.30) from

the data points collected during the decay phase. The result is an exponentially decreasing quasi-straight line with an approximate e -folding time of 0.7 year, which may not necessarily be identical to the decay time for the entire stratosphere. For comparison, *Kent and Hansen [1998]* reported an initial e -folding time of 0.8 year for the entire stratospheric layer.

Our analysis shows that the effective entire recovery time for Arctic lower stratosphere, i.e., between 12 and 16 km, is 5 years. This is also consistent with optical particle counter and satellite (Stratospheric Aerosol and Gas Experiment II) measurements at midlatitudes [*Thomason et al., 1997*]. In estimating the magnitude of the Pinatubo perturbation in the Arctic lower stratosphere, our data suggest an increase in the aerosol loading during the 1992-1993 winter to be a factor of 22 more than the pre- and post-Pinatubo background levels.

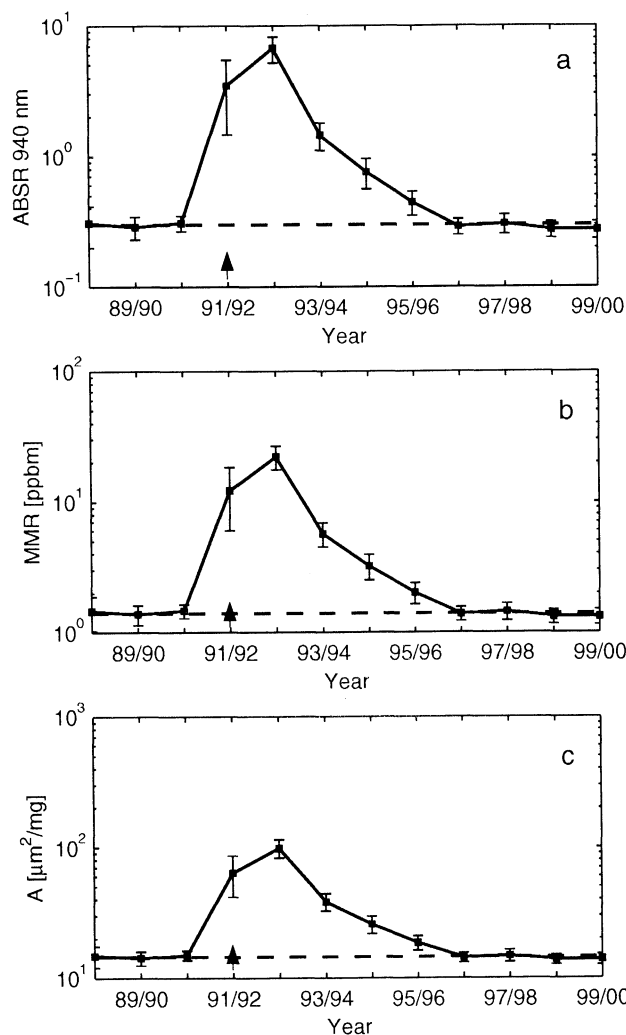


Figure 2. The seasonal averages in the range of 100-200 hPa for the (a) 940-nm aerosol backscatter ($ABSR_{940}$), (b) aerosol mass mixing ratio (MMR) (in parts per billion by mass), and (c) aerosol surface area (A) (in $\mu\text{m}^2/\text{mg}$) shown as a function of time for the period 1988-2000. The apparent pre- and post-Pinatubo background values are plotted with dashed lines as a reference for the Pinatubo perturbation; the vertical bars denote standard deviation. The winter with first observations of Pinatubo aerosol is marked with an arrow.

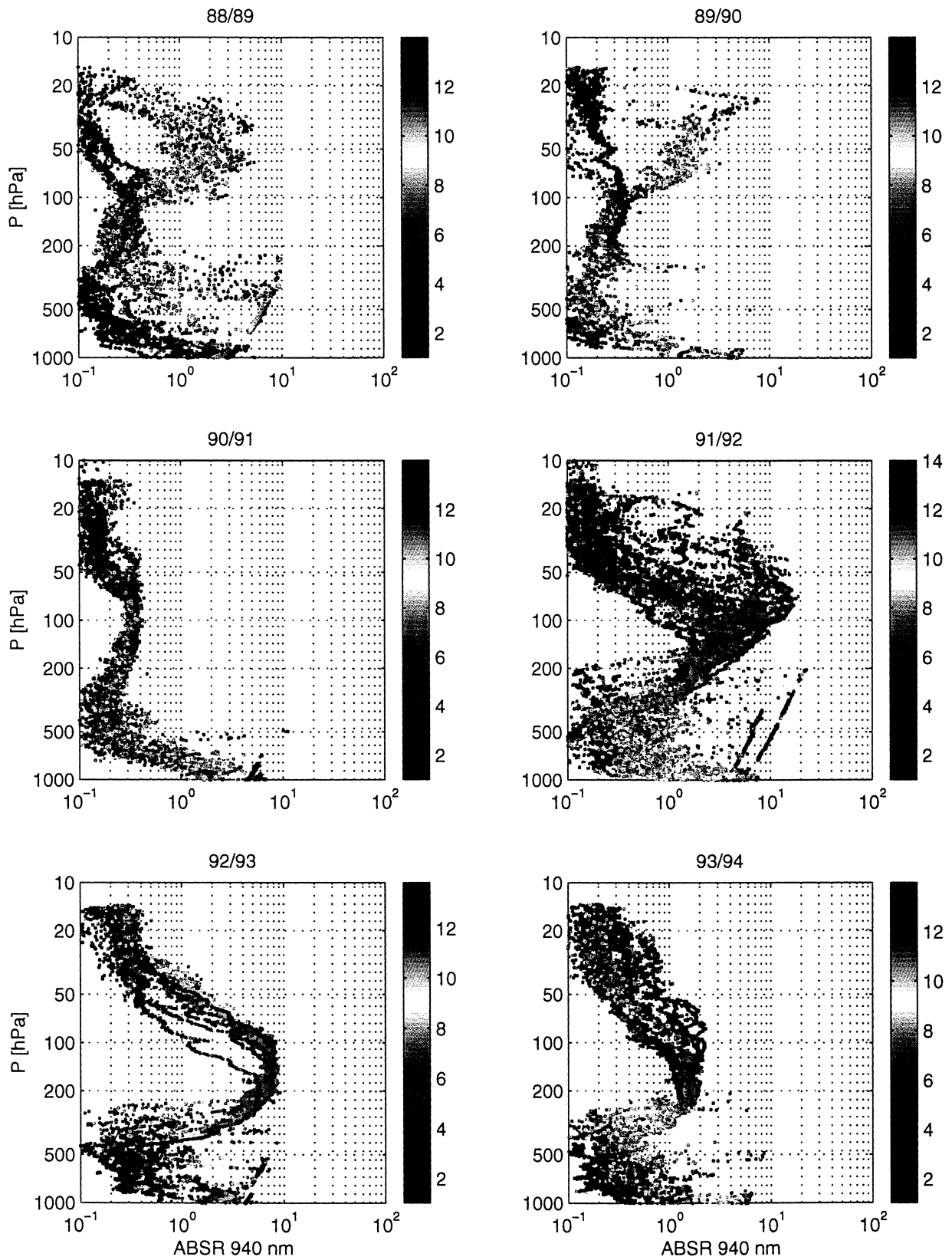


Plate 1. Vertical aerosol backscatter ratio (ABSR) and color index (CI) profiles of winters 1988-1989 to 1993-1994. In the plots the ABSR value is along the abscissa, and CI is the color of each point.

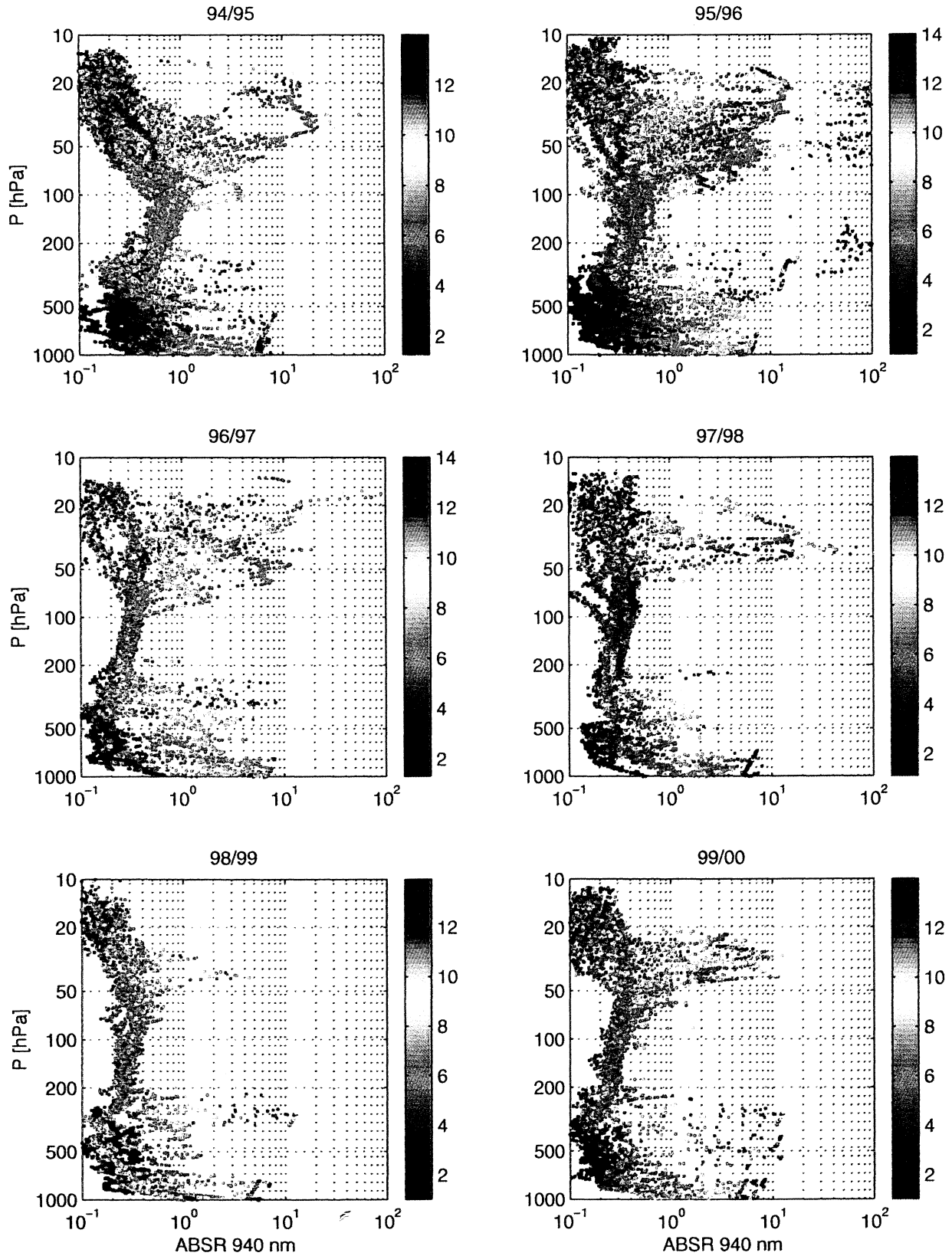


Plate 2. Vertical ABSR and CI profiles of winters 1994-1995 to 1999-2000. In the plots the ABSR value is along the abscissa, and CI is the color of each point.

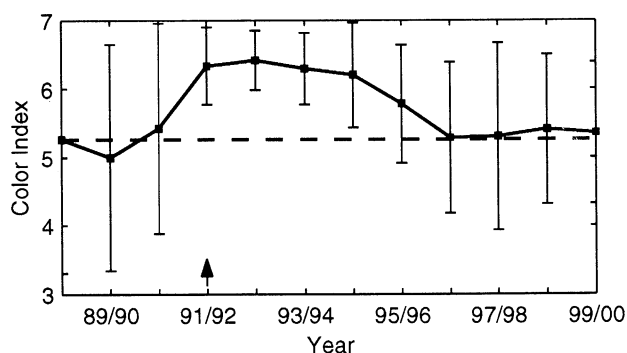


Figure 3. The seasonal averages in the range of 100-200 hPa for the color index as a function of time. The apparent pre- and post-Pinatubo background value (5.25) is plotted (dashed line) as a reference; the vertical bars denote standard deviation.

As mentioned earlier, there is also evidence of elevated CI values. The result for CI averaging is shown in Figure 3, where the seasonal averages are plotted as a function of time. Results show that the CI value is elevated during the Pinatubo perturbation. The maximum value (6.4) is recorded during the 1992-1993 winter, and the apparent background value for CI is ~ 5.3 . The notch in the background during the 1989-1990 winter most likely does not represent any anomalous meteorological condition but represents the general tendency of the calculated CI to contain increasing uncertainty with low ABSR values. Because CI is related to the size of scattering aerosols, Figure 3 illustrates the time evolution of lower stratospheric aerosol size in the lower stratosphere.

The increase in size of stratospheric aerosol particles during the Pinatubo perturbation has also been reported in earlier studies. According to *Deshler et al.* [1997] the effective particle radii (area-weighted radii) of stratospheric aerosols increased from 150 nm of pre-Pinatubo era to 550 nm during

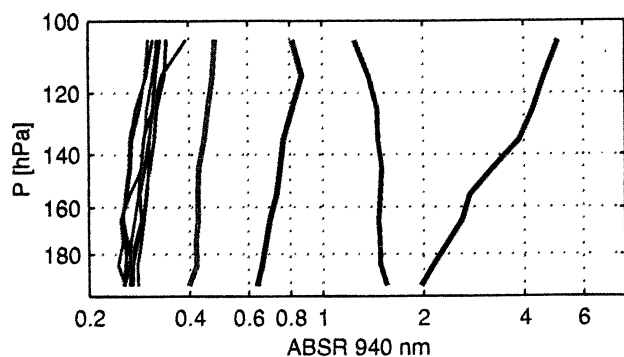


Plate 3. Partial profiles of the 940-nm aerosol backscatter ratio ($ABSR_{940}$) seasonal averages in the range of 100-200 hPa. Winters 1988-1989 to 1990-1991 (black line) indicate the background level for $ABSR_{940}$ before eruption of Mount Pinatubo; winters 1996-1997 to 1999-2000 (purple line) indicate the background after the Pinatubo event; winters during the Pinatubo event are 1991-1992 (red line), 1992-1993 (yellow line), 1993-1994 (magenta line), 1994-1995 (green line) and 1995-1996 (light blue line).

the Pinatubo perturbation and decreased back to 150-200 nm in 1997.

5. Conclusions

The results of this work suggest that backscatter sonde measurements can be used effectively in the study of long-term time development of aerosol loading in the lower stratosphere. It is obvious from the measurements that there was an elevated aerosol mixing ratio within the selected study height range of 100-200 hPa during the observed winters from 1991-1992 to 1995-1996. This phenomenon is related to the volcanic aerosol that was injected into the stratosphere in June 1991 because of the eruption of Mount Pinatubo. This Pinatubo perturbation is observed as a step change in the lower stratospheric aerosol loading, which then decays in a nearly exponential manner. We estimate here that the decay rate has an approximate e -folding time of 0.7 year, which may not necessarily be identical to the decay time for the entire stratosphere but is very near to those estimates that include the whole stratosphere [*Anderson and Saxena*, 1996; *Beyerle et al.*, 1995; *Kent and Hansen*, 1998; *Rosen et al.*, 1994].

Our measurements and calculations indicate an enhanced value of the color index (CI) during the period of elevated aerosol mass loading in the lower stratosphere following the Pinatubo eruption. This suggests an increase in particle radii.

During the pre-Pinatubo period and after the 1996-1997 winter, the study region aerosol appeared to be in a quasi steady state background condition through the 1999-2000 winter, the last year of observations reported here. The background value for the aerosol backscatter ($ABSR_{940}$) was ~ 0.30 . Background values for the aerosol mass and surface area were ~ 1 ppb and $15 \mu\text{m}^2/\text{mg}$, respectively. The maximum in seasonal averages during the Pinatubo perturbation was 6.7 for $ABSR_{940}$, 22 ppb for MMR, and $99 \mu\text{m}^2/\text{mg}$ for A. In light of these results, during the time of peak aerosol loading in the Arctic lower stratosphere 1992-1993 winter, measured aerosol backscatter ($ABSR_{940}$) was more than 22-fold, which suggest that the MMR would have been approximately 15-fold when compared with the unperturbed state. According to our calculations the increase in aerosol surface area was less dramatic. This is also in agreement with the measured increase in the particle sizes. The recovery time of the study region from the entire event was measured to be ~ 5 years.

Acknowledgments. This work was supported by Finnish Academy project Figure, European Commission Environment and Climate programme, and the United States National Science Foundation under grant OPP-9423285. Special thanks to Timo Turunen (FMI) for technical support, and Ingo Beninga (AWI), and Thomas Seiler (AWI) for making the soundings in Ny Ålesund.

References

Anderson, J., and V. Saxena, Temporal changes of Mount Pinatubo aerosol characteristics over northern midlatitudes derived from

- SAGE II extinction measurements, *J. Geophys. Res.*, *101*, 19,455–19,463, 1996.
- Beyerle, G., A. Herber, R. Neuber, and H. Gernandt, Temporal development of Mount Pinatubo aerosols as observed by lidar and sun photometer at Ny-Ålesund, Spitsbergen, *Geophys. Res. Lett.*, *22*, 2497–2500, 1995.
- Deshler, T., G. Liley, G. Bodeckerand, W. Matthews, and D. Hofmann, Stratospheric aerosol following Pinatubo: Comparison of the north and south midlatitudes using in situ measurements, *Adv. Space Res.*, *20*, 11, 2089–2095, 1997.
- International Panel on Climate Change, *Climate Change 2001: The Scientific Basis*, edited by D. Albritton, in press, 2001. (Available as <http://www.unep.ch/ipcc/index.html>)
- Kent, G., and G. Hansen, Multiwavelength lidar observations of the decay phase of stratospheric aerosol layer produced by the eruption of Mount Pinatubo in June 1991, *Appl. Opt.*, *37*, 3861–3872, 1998.
- Larsen, N., B. Knudsen, J. Rosen, N. Kjome, R. Neuber, and E. Kyrö, Temperature histories in liquid and solid polar stratospheric cloud formation, *J. Geophys. Res.*, *102*, 23,505–23,517, 1997.
- Rosen, J., and N. Kjome, Backscattersonde, a new instrument for atmospheric aerosol research, *Appl. Opt.*, *30*, 1552–1561, 1991.
- Rosen, J., N. Kjome, H. Fast, M. Khattatov, and V. Rudakov, Penetration of Mt. Pinatubo aerosols into the north polar vortex, *Geophys. Res. Lett.*, *19*, 1751–1754, 1992.
- Rosen, J., N. Kjome, and S. Oltmans, Simultaneous ozone and polar stratospheric cloud observations at South Pole Station during winter and spring 1991, *J. Geophys. Res.*, *98*, 12,741–12,751, 1993.
- Rosen, J., N. Kjome, R. McKenzie, and B. Liley, Decay of Mount Pinatubo aerosol at midlatitudes in the Northern and Southern hemispheres, *J. Geophys. Res.*, *99*, 25,733–25,739, 1994.
- Rosen, J., N. Kjome, and B. Liley, Tropospheric aerosol backscatter at a midlatitude site in the Northern and Southern hemispheres, *J. Geophys. Res.*, *102*, 21,329–21,339, 1997a.
- Rosen, J., N. Kjome, N. Larsen, B. Knudsen, E. Kyrö, R. Kivi, J. Karhu, R. Neuber, and I. Beninga, Polar stratospheric threshold temperatures in the 1995-1996 Arctic vortex, *J. Geophys. Res.*, *102*, 28,195–28,202, 1997b.
- Stevermer, A., I. Petropavlovskikh, J. Rosen, and J. DeLuisi, Development of a global stratospheric aerosol climatology: Optical properties and applications for UV, *J. Geophys. Res.*, *105*, 22,763–22,776, 2000.
- Thomason, L., L. Poole, and T. Deshler, A global climatology of stratospheric aerosol surface area deduced from Stratospheric Aerosol and Gas Experiment II measurements: 1884-1994, *J. Geophys. Res.*, *102*, 8967–8976, 1997.
- WMO, *Scientific assessment of ozone depletion: 1998. report No. 44*, World Meteorological Organization, Geneva, Switzerland, 1999.
- J. Karhu, R. Kivi, E. Kyrö, and T. Suortti Finnish Meteorological Institute, Arctic Research Centre, Tähteläntie 62, FIN-99600, Sodankylä, Finland. (tuomo.suortti@fmi.fi)
- V. Khattatov, V. Rudakov, and V. Yushkov, Central Aerological Observatory, Pervomayskaya St. Dolgoprudny, 141700 Moscow Region, Russia.
- N. Kjome and J. Rosen, Department of Physics and Astronomy, University of Wyoming, Laramie, WY 82071, USA.
- N. Larsen, Division of Middle Atmosphere Research, Danish Meteorological Institute, Lyngbyvej 100, DK-2100 Copenhagen, Denmark.
- H. Nakane, National Institute of Environmental Studies, 16-2 Onogawa, Tsukuba-Shi, Ibaraki 305-0053, Japan.
- R. Neuber, Alfred Wegner Institute, Telegrafenberg A43, D-14473 Potsdam, Germany.

(Received November 20, 2000; revised April 2, 2001; accepted April 16, 2001.)